Fearon Conor (Orcid ID: 0000-0002-8172-6094)
Olszewska Diana Angelika (Orcid ID: 0000-0002-1814-8834)
Sharma Soumya (Orcid ID: 0000-0003-3580-8504)
Fung Victor Shue Chung (Orcid ID: 0000-0003-3085-2282)
Kumar Hrishikesh (Orcid ID: 0000-0002-9789-7832)
Bhidayasiri Roongroj (Orcid ID: 0000-0002-6901-2064)

Neuroimaging Pearls from the MDS Congress Video Challenge. Part 2: Acquired Disorders

Conor Fearon MB, PhD,[1] Sapna Rawal MD,[2] Diana Olszewska MD, PhD,[1] Paula Alcaide-Leon MD,[2] Drew S. Kern MD, MS,[3] Soumya Sharma MD, DM,[4] Shyam K Jaiswal, MD, DNB,[5] Jagarlapudi MK Murthy, MD,DM, FAAN, FANS,[5] Ainhi D. Ha PhD, FRACP,[6] Raymond S. Schwartz PhD, FRACP,[7] Victor S.C. Fung PhD, FRACP,[6] Chauncey Spears MD,[8] Tracy Tholanikunnel MD,[9] Leonardo Almeida MD,[9] Taku Hatano MD,[10] Yutaka Oji MD,[10] Nobutaka Hattori MD,[10] Shantanu Shubham MD,[11] Hrishikesh Kumar MD, DM,[11] Roongroj Bhidayasiri, MD, FRCP[12,13], Christopher Laohathai, MD,[14] Anthony E. Lang MD FRCPC[1]

Affiliations:

[1] Edmond J. Safra Program in Parkinson's Disease, Morton and Gloria Shulman Movement Disorders Clinic, Toronto Western Hospital – UHN, Division of Neurology, University of Toronto, Toronto, Ontario, Canada.
[2] Division of Neuroradiology, Joint Department of Medical Imaging, Toronto Western Hospital, University Health Network, Toronto, Ontario, Canada.
[3]Department of Neurology, Departments of Neurology and Neurosurgery
University of Colorado School of Medicine, Colorado, USA.
[4] Department of Clinical Neurological Sciences, London Health Sciences Centre, Western University, London, Ontario, Canada.
[5] Department of Neurology, CARE Hospitals, Road Number 10, Banjara Hills, Hyderabad, India, 500034.
[6] Movement Disorders Unit, Westmead Hospital, Cnr Hawkesbury and Darcy Road, Westmead, NSW, 2145, Australia; Sydney Medical School, The University of Sydney, NSW, 2006, Australia.
[7] Southern Neurology, Kogarah, NSW 2145, Australia; Sydney Medical School, The University of Sydney, NSW, 2006, Australia
[8] Department of Neurology, University of Michigan, Ann Arbor, MI, US.
[9] Department of Neurology, Normal Fixel Institute for Neurological Diseases, University of Florida, Gainesville, Florida, USA
[10] Department of Neurology, Faculty of Medicine, Juntendo University, Tokyo, Japan.
[11] Institute of Neurosciences Kolkata, Kolkata, India.
[12] Chulalongkorn Centre of Excellence for Parkinson's Disease & Related Disorders, Department of Medicine, Faculty of Medicine, Chulalongkorn University and King Chulalongkorn Memorial Hospital, Thai Red Cross Society, Bangkok, 10330, Thailand
[13] The Academy of Science, The Royal Society of Thailand, Bangkok 10330, Thailand.
[14] Prasat Neurological Institute, Bangkok, Thailand.

This is the author manuscript accepted for publication and has undergone full peer review but has not been through the copyediting, typesetting, pagination and proofreading process, which may lead to differences between this version and the Version of Record. Please cite this article as doi: 10.1002/mdc3.13415

Corresponding author:

Prof. Anthony E. Lang MD, Edmond J. Safra Program in Parkinson's Disease, Morton and Gloria Shulman Movement Disorders Centre, Toronto Western Hospital, 399 Bathurst St, 7McL410, Toronto, ON, M5T 2S8 Canada

Tel: +1-416-603-5800

Fax: +1-416-603-5004

Email: Anthony.lang@uhn.ca

Word Count (abstract): 141 (Max 250)

Word Count (text): 5024 (Max 5000)

Running Title: Imaging Pearls - Acquired

Keywords: GAD65-associated disease, Sjogren syndrome, dural arteriovenous fistula, intracranial hypotension, diffuse large B cell lymphoma, toluene abuse, gnathostomiasis, MRI

Abstract:

The MDS Video Challenge continues to be the one of most widely attended sessions at the International Congress. Although the primary focus of this event is the presentation of complex and challenging cases through videos, a number of cases over the years have also presented an unusual or important neuroimaging finding related to the case. We reviewed the previous Video Challenge cases and present here a selection of those cases which incorporated such imaging findings. We have compiled these "imaging pearls" into two anthologies. The first focuses on pearls where the underlying diagnosis was a genetic condition. This second anthology focuses on imaging pearls in cases where the underlying condition was acquired. For each case we present brief clinical details along with neuroimaging findings, the characteristic imaging findings of that disorder and, finally, the differential diagnosis for the imaging findings seen.

Introduction:

Since the inaugural Video Olympics at the 2008 MDS International congress, the yearly event now known as the MDS Video Challenge continues to be the one of most popular and educational sessions at the International Congress. The event centers on the presentation of complex and challenging cases from around the world and most often the educational impact centers on the phenomenology or other clinical aspect of the history or examination and the way in which the selected experts navigate the case. Occasionally, however, these cases center on an unusual or important imaging finding which serves not to distract from the phenomenology and other clinical findings, but instead augments them, creating a rich layered picture which can be gradually revealed to the attendant audience and movement disorders experts at this highlight of the International Congress. We have therefore compiled selected "imaging pearls" from prior Video Challenge events into two anthologies. The first anthology discussed imaging pearls in which the patient had an underlying genetic condition. This second anthology will focus on unusual or important imaging findings in those Video Challenges cases where the underlying condition was acquired.

We present here 6 cases of acquired movement disorders presented at previous Video Olympics/Video Challenge events. Rather than focus on the clinical history and examination findings, the descriptions below will predominantly focus on the relevance of the neuroimaging findings to these conditions. The cases include autoimmune disorders (case 1 and 2), disorders of hemodynamics or CSF dynamics (cases 3 and 4), movement disorders secondary to neoplasia (case 5), a toxic exposure (case 6) and an infection (case 7). Each case is presented in the same format: brief details of the clinical case are presented first along with neuroimaging findings; the characteristic imaging findings of that disorder are then outlined; and finally the differential diagnosis for the imaging findings seen is discussed.

Case 1: Marked progressive cerebellar atrophy in anti-GAD antibody-associated neurological disorder

Summary of case:

A 54 year-old woman with a history of sickle cell anemia and hyperthyroidism status post radioactive iodine treatment presented with progressive dystonia and ataxia. Initial presentation was at 47 years old with sudden onset of left sided weakness, dysarthria, dysphagia and diplopia presumably from a right capsular stroke (although imaging did not show a convincing causative lesion). Months later, she developed episodic dystonic facial and right limb contractions triggered by physical activity and anxiety. On examination, she had a left hypertropia and bilateral exotropia, gaze evoked nystagmus, cerebellar dysarthria, limb dysmetria, and postural instability. Initially she was able to tandem walk with minimal assistance. Over the next few years, dystonia progressed with predominant findings of contractions of her face, jaw, hands and feet resulting in profound slowness of movement. At last follow-up, she was wheelchair bound due to profound generalized cerebellar ataxia, dystonia and spasticity.

Multiple investigations failed to provide a diagnosis until anti-GAD65 antibodies were found to be strongly positive in the serum (>1:4800) and CSF (high positive). After this result became available further questioning revealed that she had experienced episodic trunk stiffness and discomfort that had interfered with her ability to sit in her wheelchair. Examination at that time confirmed persistent excessive activity in her paraspinal and abdominal muscles.

Imaging:

Fluid-attenuated inversion recovery (FLAIR) images from MRI of the brain performed from 2007 to 2013 demonstrated progressive atrophy of the cerebellar hemispheres, with progressively increasing size of the cerebellar sulci and the fourth ventricle (Figure 1). There was also progressive volume loss of the middle cerebellar peduncles and the pons.

Characteristic imaging findings of anti-GAD65-associated disorders:

Reported imaging findings in anti-GAD65-associated disorders have been wide-ranging. These include classical T2-weighted hyperintensities in the mesial temporal lobes in the setting of autoimmune encephalitis[1] and more rarely T2-weighted hyperintensities in extralimbic areas (including thalamus, brainstem, striatum and middle cerebellar peduncle).[1,2] Generalised atrophy, cortical/subcortical T2-weighted hyperintensity and hippocampal atrophy/hyperintensity are the most common findings in anti-GAD65-associated autoimmune epilepsy.[3] Brain MRI is, however, frequently normal[4] even in the setting of cerebellar ataxia with high anti-GAD65 titres.[5] Cerebellar atrophy may, however, be present in up to 60% of patients with anti-GAD65-associated cerebellar ataxia,[6] but this tends to be mild to moderate in severity.[7] The degree of atrophy which evolved over time in this patient is unusual for an

immune-mediated cerebellar disorder. Whether this degree of cerebellar atrophy contributed to this patient's progressive dystonia, a feature infrequently seen in this disorder,[8–10] is unclear.

Differential diagnosis of imaging findings:

The differential diagnosis of preferential cerebellar atrophy includes neurodegenerative processes including hereditary ataxias and multiple system atrophy; toxic causes including exposure to alcohol, lithium, or phenytoin; post-radiation injury; chronic vertebrobasilar insufficiency; other antibody-mediated encephalopathies, which may be paraneoplastic or non-paraneoplastic; and JC virus granule cell neuronopathy.[11,12]

Case 2: Tonic spasms secondary to longitudinally extensive transverse myelitis in primary Sjogren syndrome

Summary of Case:

A 23 year-old woman presented with a one-month history of intermittent, involuntary, painful flexion of both wrists and metacarpophalangeal joints. This tonically flexed hand position, giving the appearance of clenched fists, would be maintained for 1-2 minutes and would recur 2-3 times/hour. The spasms predominantly occurred spontaneously but could also be triggered by sudden movements. Consciousness was preserved during the episodes. Two months prior to symptom onset, she presented with holocranial headaches, hiccups, and intractable vomiting. Examination revealed normal fundi, left hemi-sensory loss, bilateral brisk deep tendon reflexes, and upgoing plantars. Neuroimaging findings are discussed below. CSF aquaporin-4 antibodies were negative. Peripheral blood film demonstrated microcytic, hypochromic anemia. Further testing for inflammatory causes revealed a strongly positive anti-Ro52 antibody and a diagnosis of Sjogren syndrome was made.

Imaging:

MRI brain was unremarkable but MRI of the cervical spine revealed confluent T2 hyperintensity from C2 to C4/C5 without expansion of the cord (Figure 2).

Characteristic imaging findings in primary Sjogren syndrome:

Involvement of the nervous system in the primary Sjogren syndrome is rare, and predominantly affects the peripheral nervous system (5-15%). Involvement of the central nervous system occurs in fewer than 5% of cases.[13] Hyperintense signal changes in the deep, periventricular, and subcortical white matter (which may follow a perivascular distribution) on T2-weighted and FLAIR sequences are the most frequent MRI brain abnormalities seen in Sjogren syndrome.[14–16] Punctate contrast-enhancing foci may be present in the pons, mesencephalon, middle

cerebellar peduncles, and cerebellum.[17] Hyperintense, non-enhancing, bilateral basal ganglia, thalamic, and brainstem lesions have also been reported.[18,19]

Oher MRI brain findings described include cranial nerve involvement (e.g. optic nerve T1-weighted hyperintensity with the enhancement of the optic chiasm), bilateral temporal lobar and hippocampal T2/FLAIR hyperintensities seen in the setting of limbic encephalitis, tumefactive lesions, and marked cerebellar atrophy.[14,15,18–24] Central pontine myelinolysis, hemorrhage, lacunar infarcts, and leptomeningeal enhancement, have also been reported in some case series. [14,15,18–24]

In Sjogren-related myelopathy, spinal cord involvement typically appears as longitudinally extensive T2 hyperintensities in the posterior columns without T1 gadolinium enhancement (although enhancement has also been described).[16,22] Extensive lesions involving the entire spinal cord have also been rarely reported.[25] Sjogren's syndrome is therefore important to keep in mind in the differential of longitudinally extensive transverse myelitis (LETM).

Differential diagnosis of imaging findings:

The main imaging differential diagnosis for Sjogren syndrome is multiple sclerosis. The lesions in Sjogren syndrome are usually smaller than those in MS (although tumefactive lesions have been reported), they may affect cranial nerves, and generally do not involve the corpus callosum.[26] Larger, confluent lesions in Sjogren syndrome have to be distinguished from entities such as progressive multifocal leukoencephalopathy, acute disseminated encephalomyelitis (ADEM), lymphoma, metastases, abscesses, cysts and glioma.[26] The presence of a tumefactive lesion or multiple hyperintensities may make one consider adrenoleukodystrophy in the differential. Multiple hyperintensities in the posterior fossa, particularly when contrast-enhancing, may be concerning for vasculitis, e.g. Behçet's disease.[14,20] Tuberculosis and brain metastases are important differential diagnoses for other contrast-enhancing posterior fossa lesions.[14]

LETM involving multiple spinal segments in Sjogren syndrome may mimic neuromyelitis optica spectrum disorder (NMOSD). Aquaporin-4 antibodies are frequently positive in Sjogren syndrome and these two conditions can co-exist.[14,26] LETM may also be seen in other autoimmune inflammatory disorders (MS, ADEM or anti-MOG encephalomyelitis), systemic inflammatory disorders (Behçet's disease, systemic lupus erythematosus, antiphospholipid syndrome and sarcoidosis), infectious/parainfectious disorders (including coronavirus disease 19, tuberculosis, treponema pallidum, varicella-zoster, cytomegalovirus, Epstein Barr virus, HIV, HTLV-1, Lyme disease, schistosomiasis), neoplastic/paraneoplastic syndromes (B-cell

lymphoma, astrocytoma, ependymoma), vascular diseases (spinal cord infarction, dural arteriovenous fistula), traumatic spinal cord injury, post-radiotherapy or in nutritional deficiencies (B12, copper deficiencies).[27–30]

Case 3: Dementia and parkinsonism secondary to intracranial dural arteriovenous fistula

Summary of case:

A 64 year-old man with a 10-year history of left-sided tinnitus (noticed after minor trauma) presented with a six-month history of a progressive cognitive decline and personality change. He became apathetic, irritable, and dismissive. Three months later he became increasingly slow, unsteady, and had problems with dexterity. He was previously independent but now needed help with dressing. Family history was not contributory. Examination revealed a right-sided Horner's syndrome, scleral injection and parkinsonism. Masked facies, poverty of speech, utilization behavior, and bilateral bradykinesia (right>left) were present. His Luria test was impaired, he had a stooped posture, reduced arm swing, and postural instability.

Imaging:

MRI brain showed nonspecific FLAIR hyperintensities within the white matter of the bilateral cerebral hemispheres (Figure 3). Axial T1-weighted imaging post-gadolinium showed prominent enhancing vessels along the tentorium and within the temporo-occipital lobes bilaterally suggestive of a pseudophlebitic pattern in keeping with venous congestion. Axial T2-weighted imaging post-contrast showed corresponding prominent flow voids in keeping with venous congestion. Four vessel digital subtraction angiography showed extensive left sigmoid and transverse sinus dural AVF (dAVF), supplied by branches of vertebral arteries, ECA, tentorial branches of ICA (not shown). Embolization and ligation of the intracranial dAVF resulted in a complete resolution of symptoms.

Characteristic imaging findings of intracranial dural arteriovenous fistulae

Clinical symptoms of dAVF vary depending on the site of the fistula and the involved vessels. Dementia and parkinsonism occur relatively rarely (3-12% of cases).[31] Most cases are due to a high-grade dAVF located in the superior sagittal, transverse or sigmoid sinuses or rarely the straight sinus.[32–36] The connection with the superior sagittal sinus may result in ischemia localized to the frontal and temporal lobes and basal ganglia. [33,37]

The most common MRI brain imaging features suggestive of dAVF are diffuse T2-weighted/FLAIR hyperintensities and tortuous flow voids of venous channels.[31] While FLAIR hyperintensities are most commonly found in the white matter, they may also occur in the basal ganglia (in isolation or in combination). The hyperintensities may also be minimal or

absent.[36,38] A combination of parkinsonism and T1-weighted hyperintensities (likely related to venous congestion) in the basal ganglia is also suggestive of dAVF.[39] The signal abnormalities may fluctuate and importantly reverse with endovascular treatment.[39] Additional findings may include engorged veins, venous infarction, intracranial hemorrhage, dilated leptomeningeal or medullary vessels or vascular enhancement.[40] Dilatation of the ventricular system was described in a single case associated with dementia.[41]

Diffusion-weighted imaging (DWI) can demonstrate increased, but not restricted diffusion (secondary to venous congestion) and susceptibility-weighted imaging (SWI) can show marked dilatation and hyperintensity within the sinus/vein suggestive of arterialized flow. Time-of-flight magnetic resonance angiography may show hypertrophied feeding arteries adjacent to the fistula. [32,36,42]

The gold standard tool for diagnosis and endovascular treatment planning remains digital subtraction angiography (DSA).[32] Distinctive features may include the dAVF location at the transverse-sigmoid sinus, reflux into the straight sinus, leading to congestion of the basal ganglia and parkinsonism as in the current case.[32]

Differential diagnosis of imaging findings:

Collateral venous drainage mimicking dAVF is also an imaging feature of both acute and chronic dural thrombosis (when the proximal segment recanalizes, while the distal outflow remains obstructed in chronic dural thrombosis).[43] Other differential imaging diagnoses include cerebral arteriovenous malformations (especially pial AVM/fistula), cavernous malformations, highly vascular tumors, jugular bulb pseudo-lesions, and, in cases of a dAVF adjacent to the brainstem, an infiltrating glioma.[43,44] Finally, the confluent white matter lesions may also mimic acute leukoencephalopathy.[45]

Case 4: Hemichorea secondary to intracranial hypotension

Summary of Case:

A 35 year-old man presented with a 4-month history of decreased left-hand dexterity, specifically for holding objects and performing fine motor tasks. The symptoms progressed, with involuntary movements of the left hand emerging. He developed near-constant "fidgetiness", and these involuntary movements resulted in balance problems and falls. His past medical history included depression, ADHD and asthma. There was no history of trauma. He did not take any medications, and his family history was non-contributory.

Examination revealed a vertical supranuclear gaze palsy, absent vertical OKN, left hemichorea, brisk deep tendon reflexes with crossed adductor reflexes, non-sustained bilateral ankle clonus, and an upgoing left plantar (downgoing on the right). Coordination was impaired with tasks involving the left upper extremity, with hemichorea interfering with most movements of the left side.

Imaging:

Contrast-enhanced MRI of the brain showed inferior displacement of the brainstem, the splenium of the corpus callosum and cerebellar tonsils with associated venous distension (Figure 4). MRI of the spine showed an epidural fluid collection suggestive of a CSF leak in the thoracic region (Figure 4). Treatment with a single blood patch provided partial improvements in both balance and involuntary movement.

Characteristic imaging findings in intracranial hypotension due to spinal CSF leak:

The neuroimaging hallmark of intracranial hypotension is supra- and infratentorial pachymeningeal contrast enhancement which is found in 83% of cases.[46,47] The enhancement is typically linear, non-nodular and becomes less prevalent over time.[46–48] Spinal CSF loss leads to so-called "brain sagging" resulting from inferior displacement of the optic chiasm, cerebral aqueduct, cerebellar tonsils, and brainstem (pontomesencephalic angle <50˚, interpeduncular angle <40.5°) which can be seen in 61% of cases.[48] This can result in development of subdural hematomas or hygromas or a pressure effect on the basal ganglia and their connections and hence movement disorders (including chorea which has been reported in 3 individuals to date).[48–53]

Other features of intracranial hypotension include decreased ventricular size, effacement of the perichiasmatic/prepontine cisterns, and subarachnoid spaces.[49,54,55] Compensatory venous dilatation (a convex distention of the inferior portion of the midpoint of the dominant transverse sinus) is found in 75%, and results in the enlarged dural venous sinuses, cranial nerves, and pituitary gland (which may enhance on post-contrast MRI and may demonstrate hemorrhage within).[50,56] While MRI brain is a sensitive method of detecting intracranial hypotension (sensitivity 83%), it does not provide information on the CSF leak location and needs to be complemented by spinal MRI (94% sensitivity) and/or CT myelography.[48,49,57] The most common location of the CSF leak is the thoracic spine (41%), followed by the cervicothoracic junction (25%), cervical spine (14%), and lumbar spine (12%) (leaks may be multiple).[48,58] A CSF leak may go undetected in up to 50%.[59]

Differential diagnosis of imaging findings:

The inferior displacement of the cerebellar tonsils is a common finding in intracranial hypotension and may be mistaken for a Chiari I malformation.[60] It is important to look for other features of intracranial hypotension, in order to avoid unnecessary surgery. The engorgement of the pituitary gland may be associated with hormonal changes and may be mistaken for a pituitary adenoma (similarly risking unnecessary resection).[52] Dilatation of the inferior intercavernous sinus (suggesting a possible focal pituitary lesion), found in up to 50% of intracranial hypotension, may be seen in healthy individuals.[61] In contrast to the smooth and diffuse dural enhancement seen in intracranial hypotension, the enhancement found in metastatic/granulomatous disease or prior subdural hematoma is either nodular or irregular, or limited to one region.[62] It should be differentiated from post-lumbar puncture enhancement (seen in 5% of patients), and from infectious/carcinomatous meningitis which typically involves the leptomeninges (or neurosarcoidosis where leptomeninges are involved in up to 40%).[62,63] Collagen disorders, infections (fungal, tuberculosis, syphilis, Lyme disease), intrathecal infusions, idiopathic hypertrophic pachymeningitis, hemodialysis, ventricular shunting and leukemia/lymphoma can all also cause diffuse pachymeningeal enhancement (albeit more irregular, nodular, and thin). [49,63]

Case 5: Primary central nervous system lymphoma presenting as rapidly progressive Steele-Richardson-Olszewski syndrome

Summary of Case:

A 70-year-old man had shown abnormal behavior, bradyphrenia and a loss of verbal fluency beginning one month before presentation. On admission, there was a vertical supranuclear gaze palsy with impairment of convergence, marked facial hypomimia, hypophonia, neck and truncal rigidity and generalized bradykinesia. He had a wide-based gait with start hesitation, but he had no ataxia or tremors. Several days after admission, his level of consciousness declined. Following MRI (discussed below) a transventricular endoscopic biopsy was performed. Histological examination revealed the characteristic findings of diffuse large B-cell lymphoma (DLBL). Treatment with a course of high-dose systemic methotrexate led to improvement in the imaging abnormalities as well as his clinical symptoms.[64]

Imaging:

Figure 5 (a,b,c): Sagittal T1 post-contrast image through the midline of the brain demonstrates two avidly enhancing mass lesions, one located at the pineal gland region with involvement of the tectum, and one located within the third ventricle with involvement of the midbrain tegmentum. The third ventricular lesion is also seen on axial T2 image where it demonstrates low signal. There is extensive bilateral and symmetric edema within the globus pallidus, internal capsules, thalami, hypothalami, cerebral peduncles and midbrain on axial T2 images.

There is obstructive hydrocephalus at the level of the third ventricle with enlargement of the lateral ventricles.
Figure 5 (d,e,f): Following chemotherapy there is a marked improvement in the pre-treatment abnormalities.

Characteristic imaging findings of progressive supranuclear palsy (PSP):

The hallmark imaging feature of PSP (particularly the Richardson syndrome variant (ie PSP-RS)) is preferential atrophy of the midbrain tegmentum.[65] The resulting morphology of the tegmentum on mid-sagittal MR imaging – flattening or concave contours at the rostral and caudal aspects with elongation of the interpeduncular fossa and preservation of pontine volume – has been termed the "hummingbird" or "penguin silhouette" sign.[66,67] On axial imaging, atrophy with resulting concavity of the lateral margins of the midbrain tegmentum, with preservation of the cerebral peduncles and tectum, is referred to as the "morning glory flower sign" or "Mickey mouse" sign.[65,68] In addition to midbrain atrophy, preferential atrophy of the superior cerebellar peduncles has been documented in PSP and is thought to correlate with disease duration.[69] Large scale studies aimed at evaluating the sensitivity and specificity of these imaging features for diagnosis of PSP are challenging to perform given the need for neuropathological comparison as the gold standard for diagnosis. While the identification of typical imaging features increases diagnostic confidence for PSP, imaging remains a supportive feature rather than a major component of the diagnostic criteria.[70]

Differential diagnosis of imaging findings

Neoplastic or inflammatory disorders that may cause a PSP-like syndrome include processes that result in compression or infiltration of the brainstem, particularly those localized in the pineal region. The main differential for the imaging findings seen here is germinoma which typically involves both the pineal gland and the floor of the third ventricle. Germinomas are, however, typical of younger patients with 90% of the cases presenting before the age of 20.[71] Other differential diagnoses include high grade glioma, rosette-forming glioneuronal tumor, chordoid glioma of the third ventricle, pineal tumors with CSF dissemination and other, rarer tumors. As shown in the current case, CNS lymphoma may rarely present as a pineal region mass with low signal on T2 weighted imaging, avid enhancement, and mass effect with edema of the midbrain, thalami and basal ganglia. Differential diagnostic considerations include pineal-based tumors (pineocytoma, pineoblastoma), other extra-axial tumors that have a predilection for the pineal region (germ cell tumors, meningioma), or intra-axial tumors affecting the midbrain (glioma, metastases).[72] Inflammatory or infectious disorders such as Whipple's disease, sarcoidosis, anti-IgLON5-associated disease or neurocysticercosis may also manifest with a PSP-like presentation.[73–76]

Acknowledgement: this patient has been reported previously in a book chapter.[64]

Case 6: T2-Weighted thalamic hypointensity in the setting of toluene abuse

Summary of case:

A sixteen year-old boy presented with an 8-month history of progressive difficulty walking and imbalance with frequent falls. He was dysarthric with mild cognitive difficulty and outbursts of anger. He had normal birth and development and no prior medical history. No family members were affected.

Examination revealed interrupted pursuit with gaze-evoked horizontal nystagmus. He had a postural tremor of his right more than left upper limb in the wing beating position and an intention tremor with dysmetria, more prominent on the left than right. In addition, bilateral upper and lower limbs were spastic with upgoing plantars. His gait was ataxic.
Routine blood tests and copper studies were normal. Multiple bottles of eraser fluid (which contain toluene) were discovered in the patient's bedroom and it transpired that the duration of abuse was approximately 2 years prior to presentation.

Imaging:

MRI brain demonstrated relative hypointensity of the thalami on FLAIR and T2-weighted imaging, with a similar appearance in the dentate nuclei, as well as hyperintensity of the white matter on FLAIR/T2 imaging best seen within the posterior limbs of the internal capsules bilaterally (Figure 6). There was marked generalized atrophy of the brain parenchyma.

Characteristic imaging findings of chronic toluene abuse:

Chronic toluene abuse leads to progressive neurologic symptoms including cognitive impairment, cerebellar dysfunction, extrapyramidal features and optic neuropathy.[77] The most common imaging finding is of periventricular white matter hyperintensities of variable extent which occur in 46% of chronic abusers.[78] These may be symmetric or asymmetric and potentially reversible on discontinuation of toluene.[79,80] Corticospinal tract involvement and most notably Internal capsule hyperintensity (particularly of the posterior limb) appears to be a common finding, most likely as a result of demyelination and axonal degeneration.[81–87] Cerebral infarction and perfusion abnormalities have also been reported.[88,89] Less commonly, the cortical and deep grey matter may be involved.[90,91] Generalized cerebral atrophy, thinning of the corpus callosum and cerebellar atrophy are common.[77] Thalamic T2 hypointensity is seen in approximately 20% of patients.[78] The combination of thalamic T2 hypointensity and adjacent internal capsule hyperintensity may represent an important diagnostic clue to the abuse of this substance.[82,84,87,92,93] The "face of the giant panda sign", a characteristic finding in Wilson's disease has also been demonstrated in the setting of toluene abuse.[82] Enquiry regarding epistaxis, facial rash, behavioral changes and observing for blisters around the nose and mouth, unusual fetor, and conjunctival injection may increase diagnostic suspicion.

Differential diagnosis of imaging findings

Bilateral symmetric T2 hypointensity of the thalami is an uncommon finding that has been reported in metabolic processes such as lysosomal storage disorders[94] (specifically GM1 and GM2 gangliosidosis, Krabbe's disease, aspartylglucosaminuria, mannosidosis, fucosidosis, mucolipidosis IV, and subtypes of neuronal ceroid lipofuscinosis), aceruloplasminemia, and metachromatic leukodystrophy.[95] Acquired processes including neoplasia (e.g. lymphoma) or hemorrhage (e.g. secondary to arterial or venous infarction, or hypertension) affecting bilateral thalami may also demonstrate low T2 signal, however these processes would typically be associated with mass effect, edema or enhancement, and are less likely to be bilaterally symmetric. T2 hypointensity of grey matter is not a common finding but has been previously described.[91] T2 hypointensity in the basal ganglia most often occurs in the setting of iron deposition, and can been seen in normal aging,[96] Parkinson's disease and Huntington's disease,[97,98] multiple sclerosis,[99] Pantothenate kinase-associated neurodegeneration.[100] None of these conditions, however, with the possible exception of multiple sclerosis, typically result in concurrent T2 hypointensity within the thalamus.[91]

Confluent white matter hyperintensity involving the internal capsule can be seen most commonly in the setting of hypoglycemia[101,102] but also in amyotrophic lateral sclerosis and Krabbe disease (both of which can affect the corticospinal tracts diffusely)[103,104] and neuronal ceroid lipofuscinoses[105]. Symmetrical white matter hyperintensities involving the posterior limbs of the internal capsule and lateral brainstem are also seen in heroin vapour inhalation ("chasing the dragon").[106] Hyperintensity of the posterior limb of the internal capsule is commonly seen in amyotrophic lateral sclerosis[107] but none of the above disorders (apart from Krabbe disease) demonstrate concomitant thalamic T2 hypointensity.

Case 7: Holmes' tremor due to hemorrhagic pontine gnathostomiasis causing hypertrophic olivary degeneration

Summary of case:

A 46 year-old Thai woman developed a sudden onset of right-sided weakness and numbness with diplopia and intermittent throbbing headache 8 months previously. As the symptoms were not severe at the beginning, she did not seek any medical attention. While weakness gradually improved, she noticed abnormal movements of her right hand developing 2 months after the initial onset. No prior medical history was available. On examination, a low-frequency right-sided tremor was most noticeable in her right hand, present both at rest and with action. There was also abnormal posturing of her right fingers in association with a flexion-extension tremor of the fingers. With posture and action, tremor amplitude became more pronounced with associated overflow and right finger-to-nose ataxia. Low-frequency palatal tremor was also evident on examination. Eye movement examination demonstrated vertical pendular nystagmus. Laboratory investigations revealed elevated WBC of 10,200 with 15% of eosinophils. CSF showed no pleocytosis with normal protein and sugar. Given the imaging findings below and eosinophilia, CSF gnathostomiasis IgG Ab was tested and was positive.

Imaging:

Selected images from axial T2-weighted sequence at the level of the midbrain/pons demonstrates heterogeneous, predominantly low T2 signal abnormality with a linear morphology in the dorsal pons, preferentially localized to the left of midline (Figure 7). On coronal gradient echo sequence, there is associated blooming artifact suggestive of hemorrhage (or mineralization). There is an adjacent T2 hyperintense focus at the right pontomesencephalic junction that may represent an associated cyst or edema. Axial T2 weighted image at the level of the medulla demonstrates hypersignal and enlargement of the left inferior olivary nucleus.

Characteristic Imaging Findings of Gnathostomiasis and Hypertrophic Olivary Degeneration:

Gnathostomiasis is a parasitic infection caused by *Gnathostoma spinigerum*, which is endemic to Southeast Asia, Central and South America, and is predominantly acquired by consumption of raw freshwater fish or shellfish.[108] Several case reports and case series have described imaging findings of neurologic gnathostomiasis.[109,110] Brain imaging in affected patients has revealed several typical features, including: linear signal abnormality suggesting spread along a white-matter tract, with associated hemorrhage; multifocal hemorrhage; prominent Virchow-Robin spaces; periventricular T2 hyperintensities; brainstem involvement; and multifocal nodular enhancement in affected areas. Imaging abnormalities of the spinal cord have also been reported, specifically long-segment T2 hyperintense signal change with cord expansion consistent with myelitis. Involvement of the cauda equina has also been reported with hemorrhage, enhancement, and nerve root clumping (arachnoiditis).[111]

Hypertrophic olivary degeneration (HOD) is a unique form of neuronal degeneration most commonly resulting from a lesion along the dento-rubro-olivary pathway, also referred to as the Guillain-Mollaret triangle.[112] Cerebellar or brainstem destructive lesions, typically involving the outflow from the dentate nucleus, decussating in the midbrain around the red nucleus to the contralateral central tegmental tract result in denervation of the inferior olivary nucleus. The most common clinical manifestation is symptomatic palatal tremor; oculopalatal tremor (palatal tremor with pendular nystagmus) may also be present.[113] The characteristic MRI findings of HOD follow three phases: (1) high T2 signal within the ION without hypertrophy, generally within the first 6 months post-ictus; (2) high T2 signal and hypertrophy of the ION, lasting from 6 months to 3-4 years post-ictus; and (3) high T2 signal with resolution of hypertrophy, which can persist indefinitely.[114] This is accompanied by a brainstem or cerebellar lesion that is most commonly vascular in origin, usually hemorrhagic rather than ischemic, with a wide variety of other potential pathologies including traumatic, neoplastic, surgical, inflammatory or demyelinating.[113] Histologic studies have demonstrated macroscopic hypertrophy of the inferior olivary nuclei with corresponding neuronal swelling and vacuolization, gliosis and demyelination, ultimately leading to atrophy.[113,114] While HOD is most commonly unilateral, it may be bilateral. Bilateral HOD is also a characteristic feature of

sporadic progressive ataxia and palatal tremor (sporadic PAPT), in the absence of a structural cerebellar or brainstem lesion.[115]

Differential diagnosis of imaging findings:

As suggested above, the dorsal pontine linear signal abnormality and associated hemorrhage is consistent with gnathostomiasis. The presence of an associated pontomesencephalic cyst in addition to the elevated white cell count and eosinophilia forces other infective causes to be considered in this case. Eosinophilic meningoencephalitis may also be caused by parasitic infection with *Angiostrongylus cantonensis, Baylisascaris procyonis, o*ther helminthic parasitic infections including toxocariasis, trichinosis, cysticercosis, schistosomiasis, fascioliasis, and paragonimiasis, or fungal infection with coccidioidomycosis.[116] While neuroimaging findings of *angiostrongyliasis* and gnathostomiasis may overlap, reports suggest gnathostomiasis more commonly manifests with intracerebral hemorrhage and myelitis patterns (without clinical evidence of meningitis, as in our case), whereas angiostrongyliasis may show normal neuroimaging or abnormalities limited to the meninges.[110,117] Infection with *Baylisascaris procyonis* is less common, with several case reports describing a predilection for the periventricular white matter with FLAIR/T2 signal abnormality and enhancement evolving to chronic atrophy.[118] Imaging manifestations in neurotoxocariasis are highly variable, ranging from isolated myelitis, to multiple ring-enhancing lesions, to leptomeningeal enhancement with hydrocephalus, to vasculitis with multifocal ischemia.[119] Given the wide range of imaging manifestations of causative organisms and the possibility of significant overlap in imaging appearance, the diagnosis is generally made on the basis of clinical features, detailed exposure history, CSF and serologic testing, and potentially even tissue biopsy.

Differential diagnosis of a focal T2 hyperintense lesion with hypertrophy of the inferior olivary nucleus could include subacute vertebrobasilar perforator infarct, focal neoplasm (astrocytoma, metastasis or lymphoma), or an infectious or inflammatory process (multiple sclerosis, rhombencephalitis, sarcoidosis, etc). However, other entities may show restricted diffusion (infarct, infection) or enhancement (subacute infarct, neoplasm, active inflammation or infection), which would not be expected in HOD, and also would not follow the typical temporal progression of imaging findings expected in HOD. Additionally, the presence of an associated brainstem lesion and the typical clinical features of oculopalatal tremor would help confirm the diagnosis of HOD.

Discussion

Neuroimaging continues to be an essential paraclinical aid in the diagnosis of many movement disorders. As next generation sequencing continues to become more widely available, diagnoses in movement disorders are increasingly being made via genetic panels or whole exome sequencing approaches, often bypassing the need to exclude alternative diagnoses through an exhaustive work-up. Acquired movement disorders lack this luxury and neuroimaging remains an essential part of the diagnostic work-up for these conditions. The

cases presented here along with those presented in our accompanying anthology ("Neuroimaging Pearls from the MDS Congress Video Challenge I: Genetic Disorders") are an attempt to capture and document some of the key imaging pearls that have been presented at the MDS Video Challenge but which could easily be forgotten given the emphasis on the videotape documentation of critical phenomenology in this session.

Author Roles

1) Research project: A. Conception, B. Organization, C. Execution;
2) Statistical Analysis: A. Design, B. Execution, C. Review and Critique;
3) Manuscript: A. Writing of the first draft, B. Review and Critique.

CF 1A, 1B, 1C, 3A

SR 1A, 1B, 1C, 3B

DAO 1A, 1B, 1C, 3A

PAL 3B

DSK 3B

SS 3B

SKJ 3B

JMKM 3B

ADH 3B

RSS 3B

VSCF 3B

CS 3B

LA 3B

TH 3B

YO 3B

NH 3B

SS 3B

HK 3B

RB 3B

CL 3B

AEL 1A, 1B, 1C, 3B

Disclosures:

Funding Sources and Conflicts of Interest: The authors declare that there are no funding sources or conflicts of interest relevant to this paper.

Financial Disclosures for the previous 12 months:
CF is supported by an Edmond J. Safra Fellowship in Movement Disorders from the Michael J. Fox Foundation.
AEL reports the following: consultancies with Abbvie, Acorda, AFFiRis, Biogen, Denali, Janssen, Intracellular, Kallyope, Lundbeck, Paladin, Retrophin, Roche, Sun Pharma, Theravance, and Corticobasal Degeneration Solutions; advisory boards for Jazz Pharma, PhotoPharmics, Sunovion; honoraria from Sun Pharma, AbbVie, Sunovion, American Academy of Neurology and the International Parkinson and Movement Disorder Society; royalties from Elsevier, Saunders, Wiley-Blackwell, Johns Hopkins Press, and Cambridge University Press; and grants from Brain Canada, Canadian Institutes of Health Research, Corticobasal Degeneration Solutions, Edmond J Safra Philanthropic Foundation, Michael J. Fox Foundation, the Ontario Brain Institute, Parkinson Foundation, Parkinson Canada, and W. Garfield Weston Foundation.
All other authors have no disclosures to report.

Ethical Compliance Statement:
Informed patient consent was supplied for each case submission to the MDS Video Olympics/Video Challenge by each presenting author. The authors confirm that they have read the Journal's position on issues involved in ethical publication and affirm that this work is consistent with those guidelines.

References

1. Malter MP, Helmstaedter C, Urbach H, Vincent A, Bien CG. Antibodies to glutamic acid decarboxylase define a form of limbic encephalitis. *Ann Neurol*. 2010;67(4):470-478. doi:10.1002/ana.21917

2. Guardado Santervás PL, Arjona Padillo A, Serrano Castro P, et al. Stiff person syndrome (SPS), a basal ganglia disease? Striatal MRI lesions in a patient with SPS. *J Neurol Neurosurg Psychiatry*. 2007;78(6):657-659. doi:10.1136/jnnp.2006.099705

3. Fredriksen JR, Carr CM, Koeller KK, et al. MRI findings in glutamic acid decarboxylase associated autoimmune epilepsy. *Neuroradiology*. 2018;60(3):239-245. doi:10.1007/s00234-018-1976-6

4. Galli JR, Austin SD, Greenlee JE, Clardy SL. Stiff person syndrome with Anti-GAD65 antibodies within the national veterans affairs health administration. *Muscle Nerve*. 2018;58(6):801-804. doi:10.1002/mus.26338

5. Gordon CR, Zivotofsky AZ, Siman-Tov T, Gadoth N. Stiff person syndrome with cerebellar disease and high-titer anti-GAD antibodies. *Neurology*. 2007;68(14):1161; author reply 1161. doi:10.1212/01.wnl.0000261162.61360.a2

6. Honnorat J, Saiz A, Giometto B, et al. Cerebellar ataxia with anti-glutamic acid decarboxylase antibodies: study of 14 patients. *Arch Neurol*. 2001;58(2):225-230.

7. Baizabal-Carvallo JF. The neurological syndromes associated with glutamic acid decarboxylase antibodies. *J Autoimmun*. 2019;101:35-47. doi:10.1016/j.jaut.2019.04.007

8. Hsu YT, Duann JR, Lu MK, Sun MC, Tsai CH. Polyglandular autoimmune syndrome type 4 with GAD antibody and dystonia. *Clin Neurol Neurosurg*. 2012;114(7):1024-1026. doi:10.1016/j.clineuro.2012.01.051

9. Sunwoo JS, Chu K, Byun JI, et al. Intrathecal-specific glutamic acid decarboxylase antibodies at low titers in autoimmune neurological disorders. *J Neuroimmunol*. 2016;290:15-21. doi:10.1016/j.jneuroim.2015.11.012

10. Pittock SJ, Yoshikawa H, Ahlskog JE, et al. Glutamic acid decarboxylase autoimmunity with brainstem, extrapyramidal, and spinal cord dysfunction. *Mayo Clin Proc*. 2006;81(9):1207-1214. doi:10.4065/81.9.1207

11. Jhaveri MD, Salzman KL, Ross JS, Moore KR, Osborn AG, Ho CY. Cerebellar Atrophy. In: *Expertddx: Brain and Spine (Second Edition)*. ExpertDDx. Elsevier; 2018:522-525. doi:10.1016/B978-0-323-44308-1.50078-7

12. Wijburg MT, van Oosten BW, Murk JL, Karimi O, Killestein J, Wattjes MP. Heterogeneous imaging characteristics of JC virus granule cell neuronopathy (GCN): a case series and review of the literature. *J Neurol*. 2015;262(1):65-73. doi:10.1007/s00415-014-7530-5

13. Mekinian A, Tennenbaum J, Lahuna C, et al. Primary Sjögren's syndrome: central and peripheral nervous system involvements. *Clin Exp Rheumatol*. 2020;38 Suppl 126(4):103-109.

14. Yerdelen D, Karataş M, Alkan O, Tufan M. A new kind of and reversible brainstem involvement in primary Sjögren's syndrome as an initial manifestation. *Int J Neurosci*. 2010;120(2):155-158. doi:10.3109/00207450903359683

15. Niu B, Zou Z, Shen Y, Cao B. A case report of Sjögren syndrome manifesting bilateral basal ganglia lesions. *Medicine (Baltimore)*. 2017;96(17):e6715. doi:10.1097/MD.0000000000006715

16. Butryn M, Neumann J, Rolfes L, et al. Clinical, Radiological, and Laboratory Features of Spinal Cord Involvement in Primary Sjögren's Syndrome. *J Clin Med*. 2020;9(5):E1482. doi:10.3390/jcm9051482

17. Sakai K, Hamaguchi T, Yamada M. Multiple cranial nerve enhancement on MRI in primary Sjögren's syndrome. *Intern Med*. 2010;49(9):857-859. doi:10.2169/internalmedicine.49.3236

18. Verma R, Anand R. Limbic Encephalitis as a Heralding Manifestation of Primary Sjogren's Syndrome. *J Neurosci Rural Pract*. 2020;11(4):658-660. doi:10.1055/s-0040-1715997

19. Ararat K, Berrios I, Hannoun A, Ionete C. Case of primary Sjogren's syndrome preceded by dystonia. *BMJ Case Rep*. 2018;2018:bcr-2017-223468. doi:10.1136/bcr-2017-223468

20. Créange A, Sedel F, Brugières P, Voisin MC, Degos JD. Primary Sjögren's syndrome presenting as progressive parkinsonian syndrome. *Mov Disord*. 1997;12(1):121-123. doi:10.1002/mds.870120124

21. Kadota Y, Tokumaru AM, Kamakura K, et al. Primary Sjögren's syndrome initially manifested by optic neuritis: MRI findings. *Neuroradiology*. 2002;44(4):338-341. doi:10.1007/s00234-001-0730-6

22. Rabadi MH, Kundi S, Brett D, Padmanabhan R. Neurological pictures. Primary Sjögren syndrome presenting as neuromyelitis optica. *J Neurol Neurosurg Psychiatry*. 2010;81(2):213-214. doi:10.1136/jnnp.2009.183913

23. Wang GQ, Zhang WW. Spontaneous intracranial hemorrhage as an initial manifestation of primary Sjögren's syndrome: a case report. *BMC Neurol*. 2013;13:100. doi:10.1186/1471-2377-13-100

24. Rossi R, Valeria Saddi M. Subacute aseptic meningitis as neurological manifestation of primary Sjögren's syndrome. *Clin Neurol Neurosurg*. 2006;108(7):688-691. doi:10.1016/j.clineuro.2005.05.015

25. Verma R, Lalla R, Patil TB, Mehta V. Acute myeloneuropathy: An uncommon presentation of Sjögren's syndrome. *Ann Indian Acad Neurol*. 2013;16(4):696-698. doi:10.4103/0972-2327.120462

26. Sanahuja J, Ordoñez-Palau S, Begué R, Brieva L, Boquet D. Primary Sjögren Syndrome with tumefactive central nervous system involvement. *AJNR Am J Neuroradiol*. 2008;29(10):1878-1879. doi:10.3174/ajnr.A1204

27. Trebst C, Raab P, Voss EV, et al. Longitudinal extensive transverse myelitis--it's not all neuromyelitis optica. *Nat Rev Neurol*. 2011;7(12):688-698. doi:10.1038/nrneurol.2011.176

28. Stanifer JW, George R, Keenan RT, Massey EW. What started this? Debilitating longitudinally-extensive myelitis. *Am J Med*. 2012;125(11):1071-1073. doi:10.1016/j.amjmed.2012.07.010

29. Fumery T, Baudar C, Ossemann M, London F. Longitudinally extensive transverse myelitis following acute COVID-19 infection. *Mult Scler Relat Disord*. 2021;48:102723. doi:10.1016/j.msard.2020.102723

30. Shahriari M, Sotirchos ES, Newsome SD, Yousem DM. MOGAD: How It Differs From and Resembles Other Neuroinflammatory Disorders. *AJR Am J Roentgenol*. 2021;216(4):1031-1039. doi:10.2214/AJR.20.24061

31. Gopinath M, Nagesh C, Santhosh K, Jayadevan ER. Dementia and Parkinsonism-a Rare Presentation of Intracranial Dural Arteriovenous Fistulae. *Neurointervention*. 2017;12(2):125-129. doi:10.5469/neuroint.2017.12.2.125

32. Kwon BJ, Han MH, Kang HS, Chang KH. MR imaging findings of intracranial dural arteriovenous fistulas: relations with venous drainage patterns. *AJNR Am J Neuroradiol*. 2005;26(10):2500-2507.

33. Pu J, Si X, Ye R, Zhang B. Straight sinus dural arteriovenous fistula presenting with reversible parkinsonism: A case report and literature review. *Medicine (Baltimore)*. 2017;96(49):e9005. doi:10.1097/MD.0000000000009005

34. Chang CW, Hung HC, Tsai JI, Lee PC, Hung SC. Dural Arteriovenous Fistula With Sinus Thrombosis and Venous Reflux Presenting as Parkinsonism: A Case Report. *Neurologist*. 2019;24(4):132-135. doi:10.1097/NRL.0000000000000235

35. Velz J, Kulcsar Z, Büchele F, Richter H, Regli L. The Challenging Clinical Management of Patients with Cranial Dural Arteriovenous Fistula and Secondary Parkinson's Syndrome: Pathophysiology and Treatment Options. *Cerebrovasc Dis Extra*. 2020;10(3):124-138. doi:10.1159/000510597

36. Luo Y, Qi J, Cen Z, Hu H, Jiang B, Luo W. Two cases of dural arteriovenous fistula presenting with parkinsonism and progressive cognitive dysfunction. *J Neurol Sci*. 2014;343(1-2):211-214. doi:10.1016/j.jns.2014.05.059

37. Lai J, Heran MKS, Stoessl AJ, Gooderham PA. Reversible Parkinsonism and Rapidly Progressive Dementia Due to Dural Arteriovenous Fistula: Case Series and Literature Review. *Mov Disord Clin Pract*. 2017;4(4):607-611. doi:10.1002/mdc3.12480

38. Enofe I, Thacker I, Shamim S. Dural arteriovenous fistula as a treatable dementia. *Proc (Bayl Univ Med Cent)*. 2017;30(2):215-217. doi:10.1080/08998280.2017.11929592

39. Nogueira RG, Baccin CE, Rabinov JD, Pryor JC, Buonanno FS, Hirsch JA. Reversible parkinsonism after treatment of dural arteriovenous fistula. *J Neuroimaging*. 2009;19(2):183-184. doi:10.1111/j.1552-6569.2007.00237.x

40. Miura S, Noda K, Shiramizu N, et al. Parkinsonism and ataxia associated with an intracranial dural arteriovenous fistula presenting with hyperintense basal ganglia in T1-weighted MRI. *J Clin Neurosci*. 2009;16(2):341-343. doi:10.1016/j.jocn.2008.01.004

41. Nakahara Y, Ogata A, Takase Y, et al. Treatment of dural arteriovenous fistula presenting as typical symptoms of hydrocephalus caused by venous congestion: case report. *Neurol Med Chir (Tokyo)*. 2011;51(3):229-232. doi:10.2176/nmc.51.229

42. Fujii T, Yamadori A, Endo K, Suzuki K, Fukatsu R. Disproportionate retrograde amnesia in a patient with herpes simplex encephalitis. *Cortex*. 1999;35(5):599-614.

43. Osborn AG. Vascular Malformations. In: *Osborn's Brain*. 2nd ed. Elsevier; 2018.

44. Zyck S, De Jesus O, Gould GC. Dural Arteriovenous Fistula. In: *StatPearls*. StatPearls Publishing; 2021. Accessed July 12, 2021. http://www.ncbi.nlm.nih.gov/books/NBK532274/

45. Ikeda K, Iwasaki Y, Osako M, Ichikawa Y, Kinoshita M. Dural arteriovenous fistula mimicking leukoencephalopathy. *Neurology*. 2000;54(5):1123. doi:10.1212/wnl.54.5.1123

46. Schievink WI, Tourje J. Intracranial hypotension without meningeal enhancement on magnetic resonance imaging. Case report. *J Neurosurg*. 2000;92(3):475-477. doi:10.3171/jns.2000.92.3.0475

47. Fuh JL, Wang SJ, Lai TH, Hseu SS. The timing of MRI determines the presence or absence of diffuse pachymeningeal enhancement in patients with spontaneous intracranial hypotension. *Cephalalgia*. 2008;28(4):318-322. doi:10.1111/j.1468-2982.2007.01498.x

48. Mokri B. Cerebrospinal fluid volume depletion and its emerging clinical/imaging syndromes. *Neurosurg Focus*. 2000;9(1):e6. doi:10.3171/foc.2000.9.1.6

49. Michali-Stolarska M, Bladowska J, Stolarski M, Sąsiadek MJ. Diagnostic Imaging and Clinical Features of Intracranial Hypotension - Review of Literature. *Pol J Radiol*. 2017;82:842-849. doi:10.12659/PJR.904433

50. Watanabe A, Horikoshi T, Uchida M, Koizumi H, Yamazaki H, Kinouchi H. Subdural effusions in the posterior fossa associated with spontaneous intracranial hypotension. *Can J Neurol Sci*. 2006;33(2):205-208. doi:10.1017/s0317167100004984

51. Zwicker J, Lum C. A treatable mimic of Chiari malformation with syringomyelia. *Can J Neurol Sci*. 2009;36(4):480-482. doi:10.1017/s0317167100007824

52. Mokri B, Ahlskog JE, Luetmer PH. Chorea as a manifestation of spontaneous CSF leak. *Neurology*. 2006;67(8):1490-1491. doi:10.1212/01.wnl.0000240059.96502.bf

53. Mokri B. Movement disorders associated with spontaneous CSF leaks: a case series. *Cephalalgia*. 2014;34(14):1134-1141. doi:10.1177/0333102414531154

54. Wang DJ, Pandey SK, Lee DH, Sharma M. The Interpeduncular Angle: A Practical and Objective Marker for the Detection and Diagnosis of Intracranial Hypotension on Brain MRI. *AJNR Am J Neuroradiol*. 2019;40(8):1299-1303. doi:10.3174/ajnr.A6120

55. Figueroa EL, Jog MS, Pelz DM, Lownie SP. Spontaneous Intracranial Hypotension as a Cause of Exacerbation in Huntington's Disease. *Can J Neurol Sci*. 2018;45(3):357-359. doi:10.1017/cjn.2017.296

56. Martineau P, Chakraborty S, Faiz K, Shankar J. Imaging of the Spontaneous Low Cerebrospinal Fluid Pressure Headache: A Review. *Can Assoc Radiol J*. 2020;71(2):174-185. doi:10.1177/0846537119888395

57. Dobrocky T, Grunder L, Breiding PS, et al. Assessing Spinal Cerebrospinal Fluid Leaks in Spontaneous Intracranial Hypotension With a Scoring System Based on Brain Magnetic Resonance Imaging Findings. *JAMA Neurol*. 2019;76(5):580-587. doi:10.1001/jamaneurol.2018.4921

58. D'Antona L, Jaime Merchan MA, Vassiliou A, et al. Clinical Presentation, Investigation Findings, and Treatment Outcomes of Spontaneous Intracranial Hypotension Syndrome: A Systematic Review and Meta-analysis. *JAMA Neurol*. 2021;78(3):329-337. doi:10.1001/jamaneurol.2020.4799

59. Urbach H, Fung C, Dovi-Akue P, Lützen N, Beck J. Spontaneous Intracranial Hypotension. *Dtsch Arztebl Int*. 2020;117(27-28):480-487. doi:10.3238/arztebl.2020.0480

60. Amrhein TJ, Kranz PG. Spontaneous Intracranial Hypotension: Imaging in Diagnosis and Treatment. *Radiol Clin North Am*. 2019;57(2):439-451. doi:10.1016/j.rcl.2018.10.004

61. Alcaide-Leon P, López-Rueda A, Coblentz A, Kucharczyk W, Bharatha A, de Tilly LN. Prominent Inferior Intercavernous Sinus on Sagittal T1-Weighted Images: A Sign of Intracranial Hypotension. *AJR Am J Roentgenol*. 2016;206(4):817-822. doi:10.2214/AJR.15.14872

62. Kranz PG, Gray L, Malinzak MD, Amrhein TJ. Spontaneous Intracranial Hypotension: Pathogenesis, Diagnosis, and Treatment. *Neuroimaging Clin N Am*. 2019;29(4):581-594. doi:10.1016/j.nic.2019.07.006

63. Antony J, Hacking C, Jeffree RL. Pachymeningeal enhancement-a comprehensive review of literature. *Neurosurg Rev*. 2015;38(4):649-659. doi:10.1007/s10143-015-0646-y

64. Hatano T, Kubo SI, Hattori N, Mizuno Y. Movement disorders in neoplastic brain disease. In: *Movement Disorders in Neurologic and Systemic Disease*. Cambridge University Press; 2014:279-299.

65. Broski SM, Hunt CH, Johnson GB, Morreale RF, Lowe VJ, Peller PJ. Structural and functional imaging in parkinsonian syndromes. *Radiographics*. 2014;34(5):1273-1292. doi:10.1148/rg.345140009

66. Kato N, Arai K, Hattori T. Study of the rostral midbrain atrophy in progressive supranuclear palsy. *J Neurol Sci*. 2003;210(1-2):57-60. doi:10.1016/s0022-510x(03)00014-5

67. Oba H, Yagishita A, Terada H, et al. New and reliable MRI diagnosis for progressive supranuclear palsy. *Neurology*. 2005;64(12):2050-2055. doi:10.1212/01.WNL.0000165960.04422.D0

68. Adachi M, Kawanami T, Ohshima H, Sugai Y, Hosoya T. Morning glory sign: a particular MR finding in progressive supranuclear palsy. *Magn Reson Med Sci*. 2004;3(3):125-132. doi:10.2463/mrms.3.125

69. Tsuboi Y, Slowinski J, Josephs KA, Honer WG, Wszolek ZK, Dickson DW. Atrophy of superior cerebellar peduncle in progressive supranuclear palsy. *Neurology*. 2003;60(11):1766-1769. doi:10.1212/01.wnl.0000068011.21396.f4

70. Höglinger GU, Respondek G, Stamelou M, et al. Clinical diagnosis of progressive supranuclear palsy: The movement disorder society criteria. *Mov Disord*. 2017;32(6):853-864. doi:10.1002/mds.26987

71. Villano JL, Propp JM, Porter KR, et al. Malignant pineal germ-cell tumors: An analysis of cases from three tumor registries. *Neuro Oncol*. 2008;10(2):121-130. doi:10.1215/15228517-2007-054

72. Al-Hussaini M, Sultan I, Abuirmileh N, Jaradat I, Qaddoumi I. Pineal gland tumors: experience from the SEER database. *J Neurooncol*. 2009;94(3):351-358. doi:10.1007/s11060-009-9881-9

73. Averbuch-Heller L, Paulson GW, Daroff RB, Leigh RJ. Whipple's disease mimicking progressive supranuclear palsy: the diagnostic value of eye movement recording. *J Neurol Neurosurg Psychiatry*. 1999;66(4):532-535. doi:10.1136/jnnp.66.4.532

74. Sharma OP, Sharma AM. Sarcoidosis of the nervous system. A clinical approach. *Arch Intern Med*. 1991;151(7):1317-1321.

75. Gaig C, Graus F, Compta Y, et al. Clinical manifestations of the anti-IgLON5 disease. *Neurology*. 2017;88(18):1736-1743. doi:10.1212/WNL.0000000000003887

76. Sharma P, Garg RK, Somvanshi DS, Malhotra HS. Progressive supranuclear palsy like syndrome: neurocysticercosis an unusual cause. *Neurol India*. 2011;59(3):484-485. doi:10.4103/0028-3886.82763

77. Filley CM, Halliday W, Kleinschmidt-DeMasters BK. The effects of toluene on the central nervous system. *J Neuropathol Exp Neurol*. 2004;63(1):1-12. doi:10.1093/jnen/63.1.1

78. Aydin K, Sencer S, Demir T, Ogel K, Tunaci A, Minareci O. Cranial MR findings in chronic toluene abuse by inhalation. *AJNR Am J Neuroradiol*. 2002;23(7):1173-1179.

79. Kobayashi M. Marked asymmetry of white matter lesions caused by chronic toluene exposure. *Neurol Sci*. 2014;35(3):495-497. doi:10.1007/s10072-013-1581-8

80. Lin CM, Liu CK. Reversible cerebral periventricular white matter changes with corpus callosum involvement in acute toluene-poisoning. *J Neuroimaging*. 2015;25(3):497-500. doi:10.1111/jon.12155

81. Ramcharan K, Ramesar A, Ramdath M, Teelucksingh J, Gosein M. Encephalopathy and Neuropathy due to Glue, Paint Thinner, and Gasoline Sniffing in Trinidad and Tobago-MRI Findings. *Case Rep Neurol Med*. 2014;2014:850109. doi:10.1155/2014/850109

82. Video Tournament. A case of progressive gait imbalance. Presented at: June 4, 2021; 7th Asian and Oceanian Parkinson's Disease and Movement Disorders Congress.

83. Ikeda M, Tsukagoshi H. Encephalopathy due to toluene sniffing. Report of a case with magnetic resonance imaging. *Eur Neurol*. 1990;30(6):347-349. doi:10.1159/000117371

84. Hirai H, Ikeuchi Y. [MRI of chronic toluene intoxication]. *Rinsho Shinkeigaku*. 1993;33(5):552-555.

85. Terashi H, Nagata K, Satoh Y, Hirata Y, Hatazawa J. [Hippocampal hypoperfusion underlying dementia due to chronic toluene intoxication]. *Rinsho Shinkeigaku*. 1997;37(11):1010-1013.

86. Sakai T, Honda S, Kuzuhara S. [Encephalomyelopathy demonstrated on MRI in a case of chronic toluene intoxication]. *Rinsho Shinkeigaku*. 2000;40(6):571-575.

87. Kojima S, Hirayama K, Furumoto H, Fukutake T, Hattori T. [Magnetic resonance imaging in chronic toluene abuse, and volitional hyperkinesia]. *Rinsho Shinkeigaku*. 1993;33(5):477-482.

88. Marey-López J, Rubio-Nazabal E, Alonso-Magdalena L, López-Facal S. Cerebral infarction after toluene inhalation. *Cerebrovasc Dis*. 2003;16(1):107-108. doi:10.1159/000070128

89. Ryu YH, Lee JD, Yoon PH, Jeon P, Kim DI, Shin DW. Cerebral perfusion impairment in a patient with toluene abuse. *J Nucl Med*. 1998;39(4):632-633.

90. Caldemeyer KS, Armstrong SW, George KK, Moran CC, Pascuzzi RM. The spectrum of neuroimaging abnormalities in solvent abuse and their clinical correlation. *J Neuroimaging*. 1996;6(3):167-173. doi:10.1111/jon199663167

91. Kamran S, Bakshi R. MRI in chronic toluene abuse: low signal in the cerebral cortex on T2-weighted images. *Neuroradiology*. 1998;40(8):519-521. doi:10.1007/s002340050637

92. Sodeyama N, Orimo S, Okiyama R, Arai M, Tamaki M. [A case of chronic thinner intoxication developing hyperkinésie volitionnelle three years after stopping thinner abuse]. *Rinsho Shinkeigaku*. 1993;33(2):213-215.

93. Suzuki Y, Oishi M, Ogawa K, Kamei S. A patient with Marchiafava-Bignami disease as a complication of diabetes mellitus treated effectively with corticosteroid. *J Clin Neurosci*. 2012;19(5):761-762. doi:10.1016/j.jocn.2011.07.040

94. Autti T, Joensuu R, Aberg L. Decreased T2 signal in the thalami may be a sign of lysosomal storage disease. *Neuroradiology*. 2007;49(7):571-578. doi:10.1007/s00234-007-0220-6

95. Martin A, Sevin C, Lazarus C, Bellesme C, Aubourg P, Adamsbaum C. Toward a better understanding of brain lesions during metachromatic leukodystrophy evolution. *AJNR Am J Neuroradiol*. 2012;33(9):1731-1739. doi:10.3174/ajnr.A3038

96. Drayer B, Burger P, Darwin R, Riederer S, Herfkens R, Johnson GA. MRI of brain iron. *AJR Am J Roentgenol*. 1986;147(1):103-110. doi:10.2214/ajr.147.1.103

97. Stern MB, Braffman BH, Skolnick BE, Hurtig HI, Grossman RI. Magnetic resonance imaging in Parkinson's disease and parkinsonian syndromes. *Neurology*. 1989;39(11):1524-1526. doi:10.1212/wnl.39.11.1524

98. Chen JC, Hardy PA, Kucharczyk W, et al. MR of human postmortem brain tissue: correlative study between T2 and assays of iron and ferritin in Parkinson and Huntington disease. *AJNR Am J Neuroradiol*. 1993;14(2):275-281.

99. Russo C, Smoker WR, Kubal W. Cortical and subcortical T2 shortening in multiple sclerosis. *AJNR Am J Neuroradiol*. 1997;18(1):124-126.

100. Savoiardo M, Halliday WC, Nardocci N, et al. Hallervorden-Spatz disease: MR and pathologic findings. *AJNR Am J Neuroradiol*. 1993;14(1):155-162.

101. Albayram S, Ozer H, Gokdemir S, et al. Reversible reduction of apparent diffusion coefficient values in bilateral internal capsules in transient hypoglycemia-induced hemiparesis. *AJNR Am J Neuroradiol*. 2006;27(8):1760-1762.

102. Nakajima N, Ueda M, Nagayama H, Katayama Y. Hypoglycemia-induced spontaneous unilateral jerking movement in bilateral internal capsule posterior limb abnormalities. *J Neurol Sci*. 2014;338(1-2):220-222. doi:10.1016/j.jns.2013.12.041

103. Cousyn L, Law-Ye B, Pyatigorskaya N, et al. Brain MRI features and scoring of leukodystrophy in adult-onset Krabbe disease. *Neurology*. 2019;93(7):e647-e652. doi:10.1212/WNL.0000000000007943

104. Jin J, Hu F, Zhang Q, Jia R, Dang J. Hyperintensity of the corticospinal tract on FLAIR: A simple and sensitive objective upper motor neuron degeneration marker in clinically verified amyotrophic lateral sclerosis. *J Neurol Sci*. 2016;367:177-183. doi:10.1016/j.jns.2016.06.005

105. Biswas A, Krishnan P, Amirabadi A, Blaser S, Mercimek-Andrews S, Shroff M. Expanding the Neuroimaging Phenotype of Neuronal Ceroid Lipofuscinoses. *AJNR Am J Neuroradiol*. 2020;41(10):1930-1936. doi:10.3174/ajnr.A6726

106. Kriegstein AR, Shungu DC, Millar WS, et al. Leukoencephalopathy and raised brain lactate from heroin vapor inhalation ("chasing the dragon"). *Neurology*. 1999;53(8):1765-1773. doi:10.1212/wnl.53.8.1765

107. Protogerou G, Ralli S, Tsougos I, et al. T2 FLAIR Increased Signal Intensity at the Posterior Limb of the Internal Capsule: Clinical Significance in ALS Patients. *Neuroradiol J*. 2011;24(2):226-234. doi:10.1177/197140091102400210

108. Herman JS, Chiodini PL. Gnathostomiasis, another emerging imported disease. *Clin Microbiol Rev*. 2009;22(3):484-492. doi:10.1128/CMR.00003-09

109. Sawanyawisuth K, Tiamkao S, Kanpittaya J, Dekumyoy P, Jitpimolmard S. MR imaging findings in cerebrospinal gnathostomiasis. *AJNR Am J Neuroradiol*. 2004;25(3):446-449.

110. Kanpittaya J, Sawanyawisuth K, Intapan PM, Khotsri P, Chotmongkol V, Maleewong W. A comparative study of neuroimaging features between human neuro-gnathostomiasis and angiostrongyliasis. *Neurol Sci*. 2012;33(4):893-898. doi:10.1007/s10072-011-0864-1

111. Sawanyawisuth K, Tiamkao S, Nitinavakarn B, Dekumyoy P, Jitpimolmard S. MR imaging findings in cauda equina gnathostomiasis. *AJNR Am J Neuroradiol*. 2005;26(1):39-42.

112. Guillain G. *Deux cas de myoclonies synchrones et rythmées vélo-pharyngo-laryngo-oculo-diaphragmatiques. Le problème anatomique et physio-pathologique de ce syndrome*. Masson; 1932.

113. Tilikete C, Desestret V. Hypertrophic Olivary Degeneration and Palatal or Oculopalatal Tremor. *Front Neurol*. 2017;8:302. doi:10.3389/fneur.2017.00302

114. Goyal M, Versnick E, Tuite P, et al. Hypertrophic olivary degeneration: metaanalysis of the temporal evolution of MR findings. *AJNR Am J Neuroradiol*. 2000;21(6):1073-1077.

115. Samuel M, Torun N, Tuite PJ, Sharpe JA, Lang AE. Progressive ataxia and palatal tremor (PAPT): clinical and MRI assessment with review of palatal tremors. *Brain*. 2004;127(Pt 6):1252-1268. doi:10.1093/brain/awh137

116. Weller PF. Eosinophilic meningitis. *Am J Med*. 1993;95(3):250-253. doi:10.1016/0002-9343(93)90275-t

117. Kanpittaya J, Jitpimolmard S, Tiamkao S, Mairiang E. MR findings of eosinophilic meningoencephalitis attributed to Angiostrongylus cantonensis. *AJNR Am J Neuroradiol*. 2000;21(6):1090-1094.

118. Rowley HA, Uht RM, Kazacos KR, et al. Radiologic-pathologic findings in raccoon roundworm (Baylisascaris procyonis) encephalitis. *AJNR Am J Neuroradiol*. 2000;21(2):415-420.

119. Sánchez SS, García HH, Nicoletti A. Clinical and Magnetic Resonance Imaging Findings of Neurotoxocariasis. *Front Neurol*. 2018;9:53. doi:10.3389/fneur.2018.00053

Legends

Figure 1. Case 1: Sequential axial FLAIR images demonstrating progressive atrophy of cerebellar hemispheres, prominence of cerebellar sulci and fourth ventricle and volume loss in middle cerebellar peduncle and pons.

Figure 2: Case 2: Axial and sagittal T2 imaging of the brain demonstrates normal appearance of the grey and white matter. In particular, the corpus callosum is unremarkable. Sagittal T2 imaging of the cervical spine demonstrates hypersignal within the cord, extending from the mid-C2 level to the C4-5 level (>2 vertebral bodies in length). There is no significant cord expansion.

Figure 3. Case 3: Axial FLAIR MRI brain at the level of the basal ganglia (a), the corona radiata (b); gadolinium-enhanced T1-weighted imaging showing enhancement of engorged vessels (dashed arrows) (c); axial T2-weighted imaging with gadolinium showing small flow voids anterior to the brainstem and in the right temporal lobe from engorged vessels (small arrows), and large flow void from dilatation of the torcula, right transverse and sigmoid sinuses (large arrows) (d).

Figure 4. Case 4: Axial T2 FLAIR MRI brain (a,b) and contrast-enhanced sagittal T1 (c) showing inferior displacement of the brainstem, splenium of the corpus callosum and cerebellar tonsils with associated venous distension. Axial T2 post-contrast MRI spine at the T6 level (d) demonstrating an epidural fluid collection suggestive of CSF leak.

Figure 5. Case 5: (a,b,c): Pretreatment axial T2 and sagittal T1 post-contrast images demonstrating two avidly enhancing mass lesions and extensive bilateral and symmetric edema within the globus pallidus, internal capsules, thalami, hypothalamus, midbrain and cerebral peduncles with obstructive hydrocephalus (see text for details) (d,e,f): Post-chemotherapy axial T2 and sagittal T1 post-contrast images demonstrating marked improvement in the pre-treatment abnormalities.

Figure 6. Case 6: Axial FLAIR (a), axial T2-weighted imaging (b) and coronal T2-weighted imaging (c) demonstrating hypointensity of thalami bilaterally and hyperintensity of the white matter (most notably of the posterior limbs of the internal capsules) and marked generalized atrophy. Coronal T2-weighted imaging through the dentate nuclei (d) shows similar hypointensities in the dentate nuclei.

Figure 7. Case 7: Axial T2-weighted images demonstrating focal area of predominantly T2 hypointensity in the left midbrain and pons (see text for details) (a-e); coronal gradient echo sequence demonstrating associated blooming artefact (f); g: axial T2-weighted image at the level of the inferior olive showing olivary hypertrophy and hyperintensity (hatched arrow).

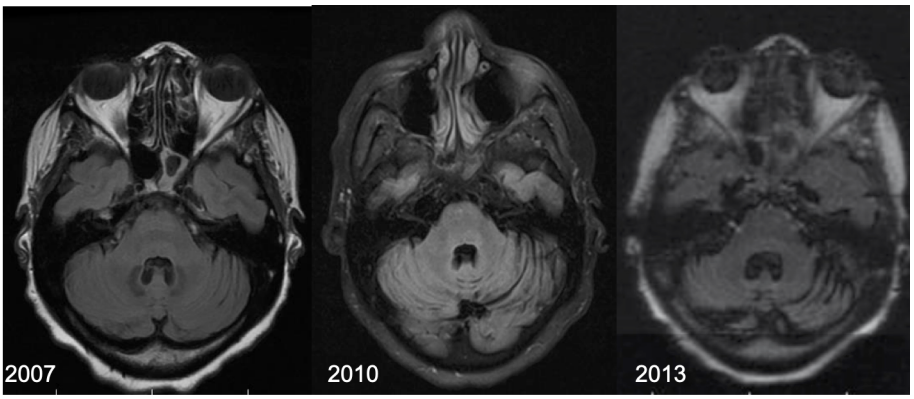

MDC3_13415_Figure1orig300.tiff

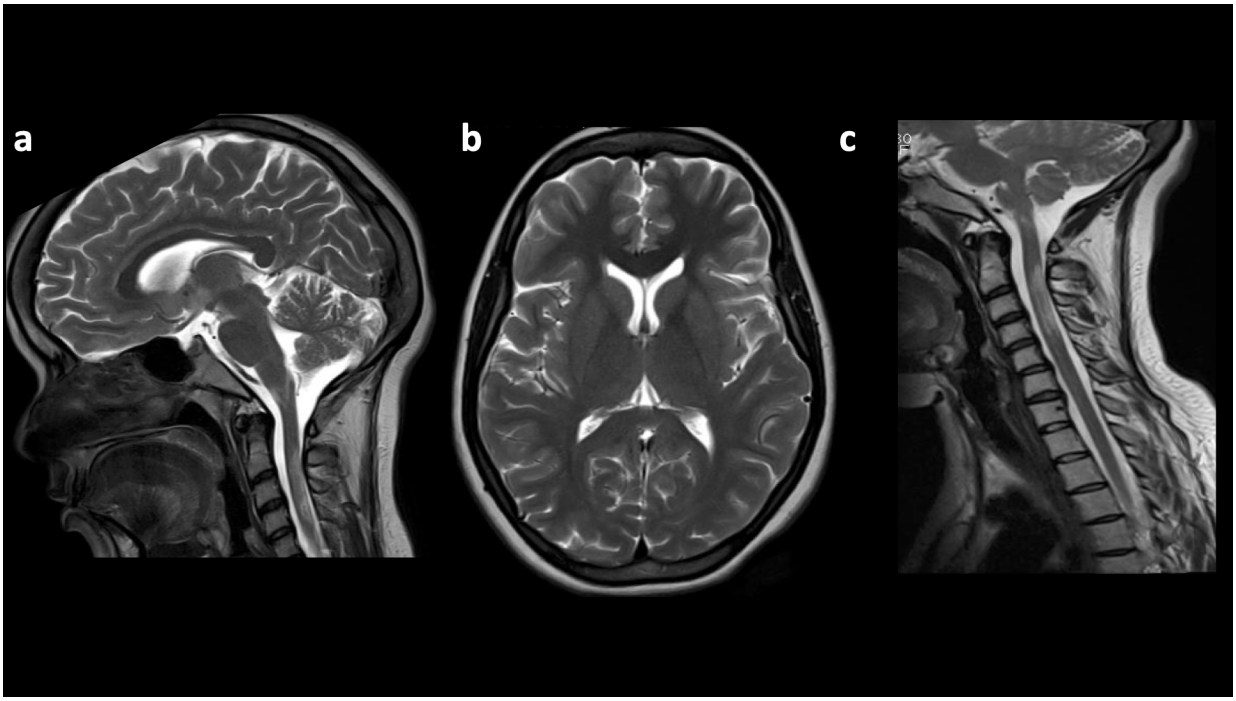

MDC3_13415_Figure2orig300.tiff

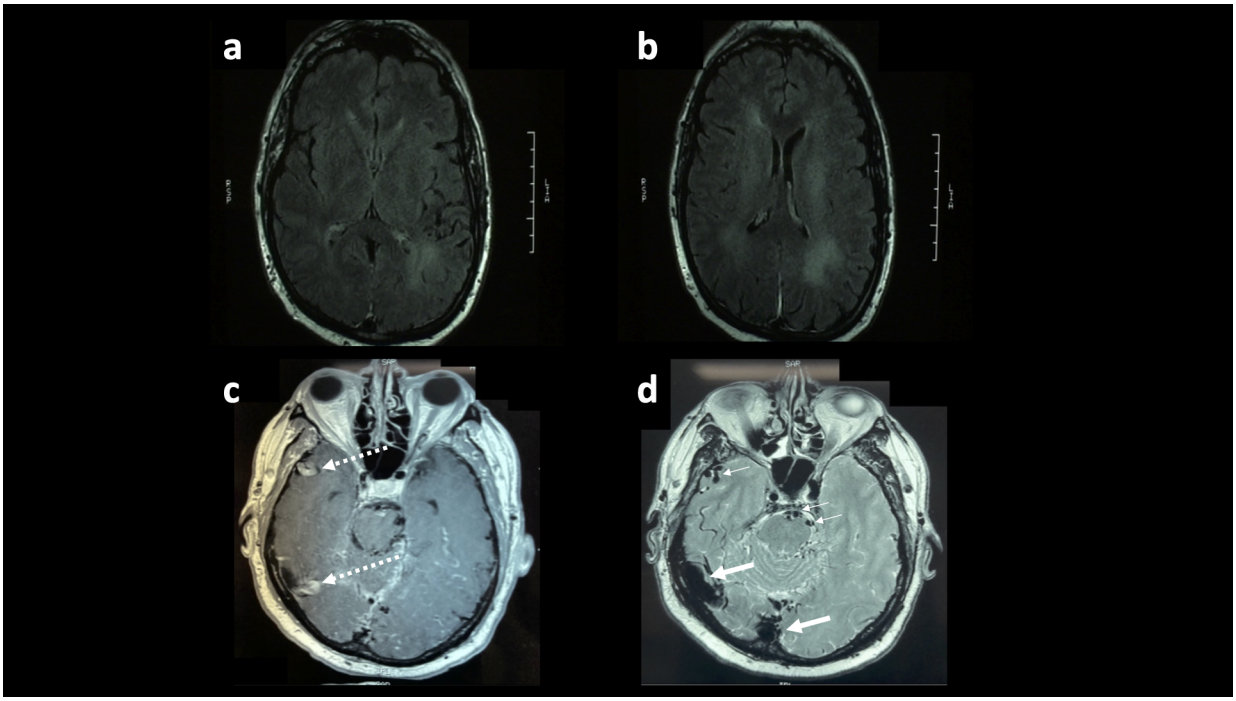

MDC3_13415_Figure3orig300.tiff

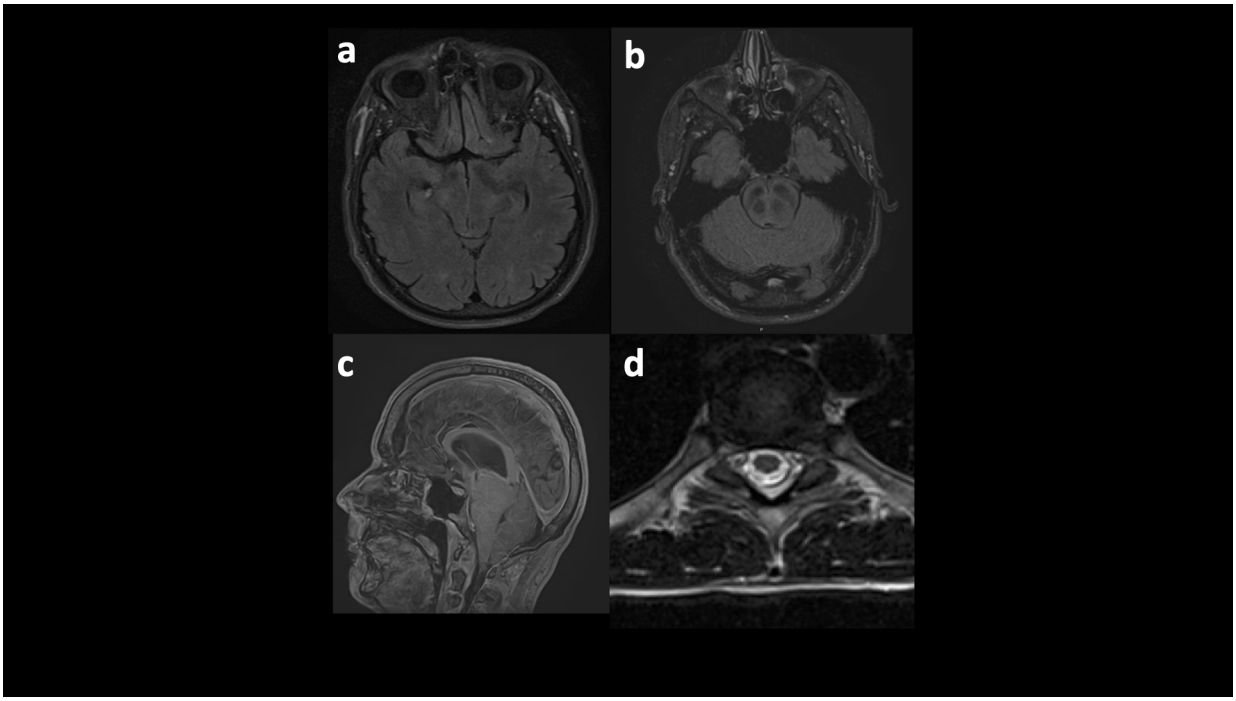

MDC3_13415_Figure4orig300.tiff

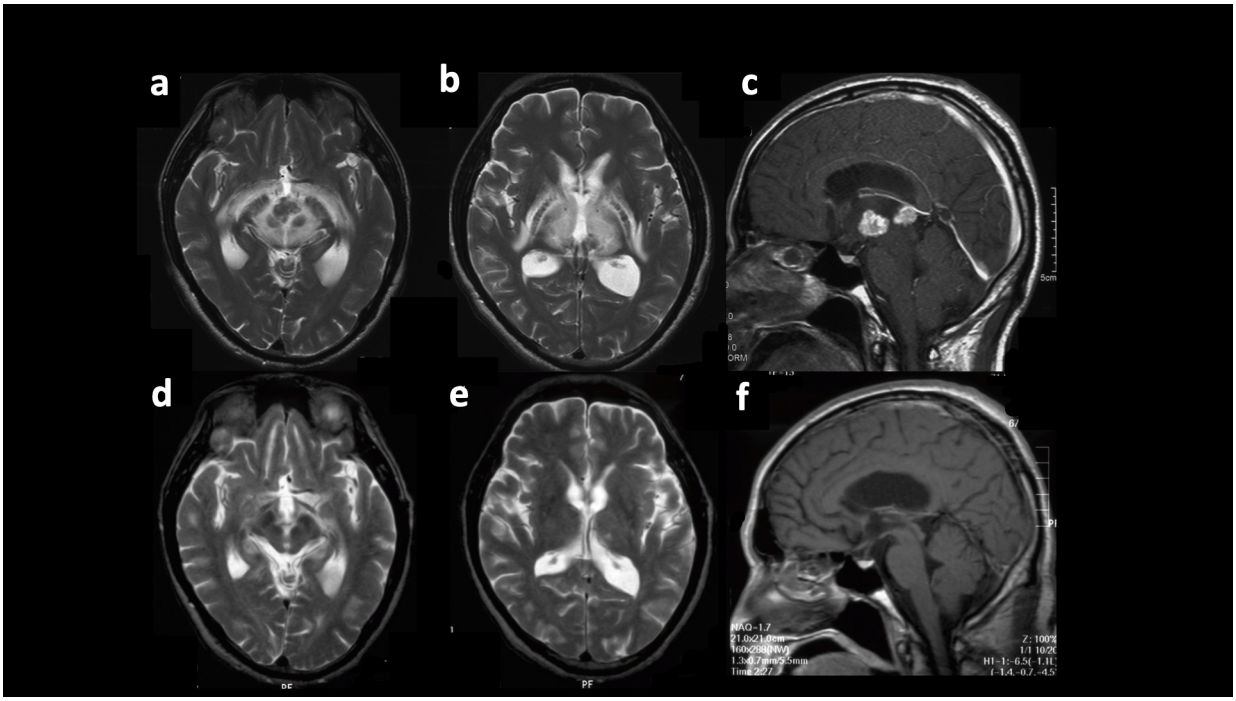

MDC3_13415_Figure5orig300.tiff

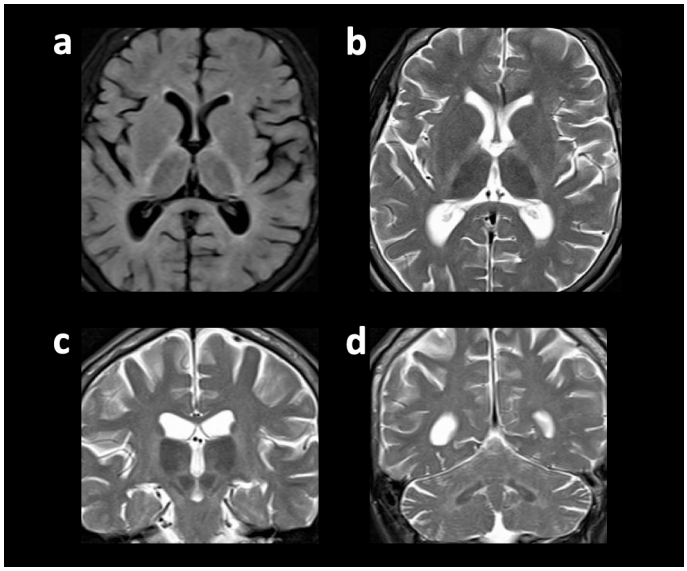

MDC3_13415_Figure6orig300.tiff

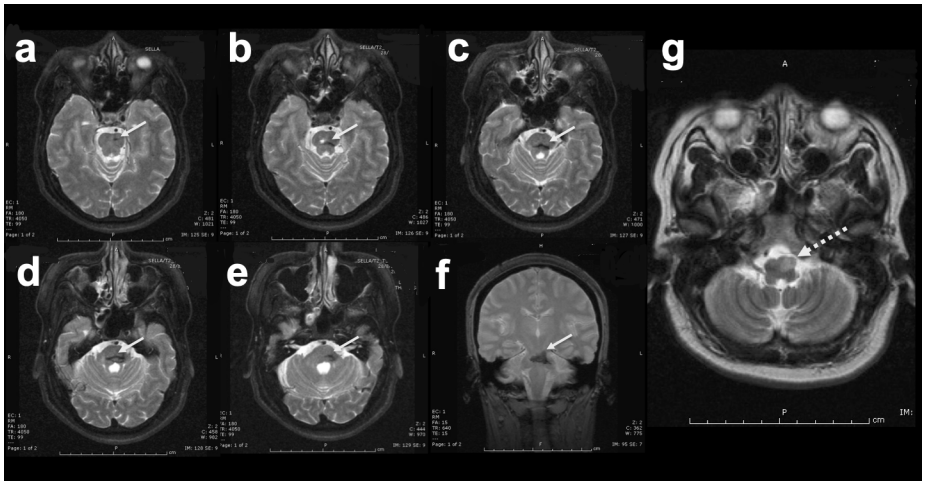

MDC3_13415_Figure7orig300.tiff